

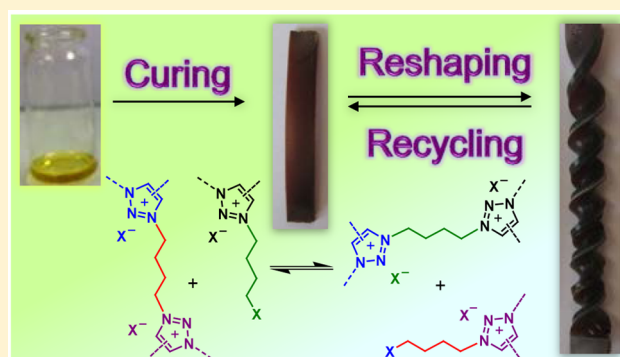
Reprocessing and Recycling of Highly Cross-Linked Ion-Conducting Networks through Transalkylation Exchanges of C–N Bonds

Mona M. Obadia, Bhanu P. Mudraboyina, Anatoli Serghei, Damien Montarnal,* and Eric Drockenmüller*

Université Claude Bernard Lyon 1, INSA de Lyon, Ingénierie des Matériaux Polymères (UMR CNRS 5223), 15 Boulevard Latarjet, Villeurbanne Cedex 69622, France

Supporting Information

ABSTRACT: Exploiting exchangeable covalent bonds as dynamic cross-links recently afforded a new class of polymer materials coined as vitrimers. These permanent networks are insoluble and infusible, but the network topology can be reshuffled at high temperatures, thus enabling glasslike plastic deformation and reprocessing without depolymerization. We disclose herein the development of functional and high-value ion-conducting vitrimers that take inspiration from poly(ionic liquid)s. Tunable networks with high ionic content are obtained by the solvent- and catalyst-free polyaddition of an α -azide- ω -alkyne monomer and simultaneous alkylation of the resulting poly(1,2,3-triazole)s with a series of difunctional cross-linking agents. Temperature-induced transalkylation exchanges of C–N bonds between 1,2,3-triazolium cross-links and halide-functionalized dangling chains enable recycling and reprocessing of these highly cross-linked permanent networks. They can also be recycled by depolymerization with specific solvents able to displace the transalkylation equilibrium, and they display a great potential for applications that require solid electrolytes with excellent mechanical performances and facile processing such as supercapacitors, batteries, fuel cells, and separation membranes.



INTRODUCTION

Covalently cross-linked networks or thermosetting materials offer considerable advantages over thermoplastics, such as solvent resistance and improved thermomechanical properties. Their key benefit, that is, maintaining a permanent and intractable three-dimensional structure, also constitutes the major drawback of these materials, since they cannot be recycled or reprocessed. Such properties clearly distinguish them from thermoplastics constituted by individual chains that are soluble, reprocessable, and display a melt viscosity. Numerous combinations of these two polymer classes taking advantage of phase separation, crystallization, or weak interactions have enabled over the years high-throughput processing of materials displaying excellent mechanical and solvent-resistance properties. Reversible cross-linking with covalent chemistry or supramolecular interactions has allowed to some extent the switch from properties of thermosets to thermoplastics by heat, light, or other stimuli.^{1–8} The variations of viscosity with temperature can thus be amplified by several orders of magnitude in comparison to classical thermoplastics.

A novel paradigm that features a constant reshuffling of covalent cross-links by covalent exchange reactions has been recently proposed.^{9–11} In contrast to covalent and noncovalent reversible bonds that are disrupted and re-cross-linked upon changes in temperature, a concerted exchange mechanism between cross-links permits reorganization of the network topology and stress relief while maintaining at all times the

cross-linking density at a constant level. The temperature dependence of viscosity in such materials is controlled by the kinetics of the chemical exchange reaction and is greatly reduced when compared to linear polymers. Such materials also known as vitrimers can therefore be reprocessed without any precise temperature control, following simple techniques inspired from glass smithing, that is, bending, twisting, and blowing. A limited number of covalent exchange reactions^{12,13} have demonstrated the concept of vitrimers and covalent adaptable networks. These examples include transesterification and transamination reactions,^{14–20} as well as metatheses of olefins^{21,22} or siloxanes.²³ Except from transamination reactions, most of these examples require the presence of catalysts in order to accelerate the exchange rates and to adapt the macroscopic stress relaxation of the material to application-relevant time scales and temperatures.

We have recently reported on poly(1,2,3-triazolium ionic liquid)s (PTILs) as a promising new class of ion-conducting polymer materials.²⁴ Their modular nature builds on the robust, efficient, and orthogonal attributes of the copper-catalyzed alkyne–azide cycloaddition (CuAAC) as well as on the quantitative alkylation of 1,2,3-triazoles and the large tunability of counteranions offered by anion metathesis. Moreover, PTILs can be easily obtained in a one-step process by thermal azide–

Received: March 12, 2015

Published: April 15, 2015

alkyne 1,3-dipolar cycloaddition followed by in situ alkylation of the resulting poly(1,2,3-triazole)s with a suitable quaternizing agent.²⁵ These linear PTILs synthesized without a copper catalyst and containing a statistical sequence of 1,3,4- and 1,3,5-trisubstituted 1,2,3-triazoliums have properties comparable to their regioisomeric 1,3,4-trisubstituted analogues. This versatile solvent- and catalyst-free approach is extended herein to the formation of ion-conducting networks. Remarkably, such permanently cross-linked networks behave as vitrimers, and we describe here rheological studies of the networks corroborated by NMR experiments with model compounds that point to a C–N bond transalkylation exchange on the 1,2,3-triazolium groups as the origin of this behavior.

RESULTS AND DISCUSSION

One-pot poly(1,2,3-triazolium) networks were obtained from the curing of stoichiometric amounts of azide, alkyne, and quaternizing groups by using self-condensing α -azide- ω -alkyne monomer **1** and 1,6-dibromohexane difunctional cross-linker **2** ($X = 2[2]/[1] = 1.0$). This unprecedented approach constitutes a very practical and highly tunable process to manufacture thermosetting materials with high ionic content and with negligible amount of soluble constituents. In contrast to previously described cross-linked poly(ionic liquid)s,²⁶ this approach does not require any catalyst, polymerization mediator, or solvent, and materials with different shapes and thicknesses ranging from 100 μm to several centimeters can be readily obtained (Figure 1).

The reaction kinetics of this thermally curable system were monitored by ¹H NMR using a model system, in which **2** was replaced by 1-bromooctane to avoid cross-linking (Figures S1 and S2, Supporting Information). The evolution of the different species shows as expected the simultaneous consumption of azide and alkyne functionalities and the concomitant generation of 1,2,3-triazoles, followed soon after by their quaternization into 1,2,3-triazoliums. This indicates that the polyaddition and the quaternization reactions proceed at similar rates at 110 °C. In terms of macromolecular architecture, the consequences are that the covalent networks are formed by the successive growth of branched ionic clusters followed by sudden condensation into a percolated ion-conducting network. Rheometry monitoring of network formation at 110 °C using **2** as the cross-linker (Figure S3, Supporting Information) shows a dramatic increase of elastic (G') and loss (G'') moduli in the vicinity of the gelation time (t_{gel} corresponds to the G'/G'' crossover occurring at approximately 40 min). In the following, the curing times were set to 48 h at 110 °C to ensure a complete curing of the system.

Determining the actual composition of the ionic network (i.e., the fractions of 1,2,3-triazole, 1,2,3-triazolium, and bromide groups) proved challenging as no significant shifts could be noticed on Fourier transform IR spectra upon curing, and the low swelling excludes the use of high-resolution magic angle spinning (HR-MAS) NMR spectroscopy. The only technique that successfully allowed estimation of the network composition was X-ray photoelectron spectroscopy (XPS). Detailed analysis of the high-resolution N_{1s} spectra allowed quantification of the ratio of 1,2,3-triazolium and 1,2,3-triazole groups at the extreme surface (approximately 10 nm) of samples taken at different depths inside the PTIL network (Figure S4, Supporting Information). Statistical analysis of the different species gave as composition of the cured network 9.0 wt % of linear 1,2,3-triazole segments, 24 wt % of 1,2,3-

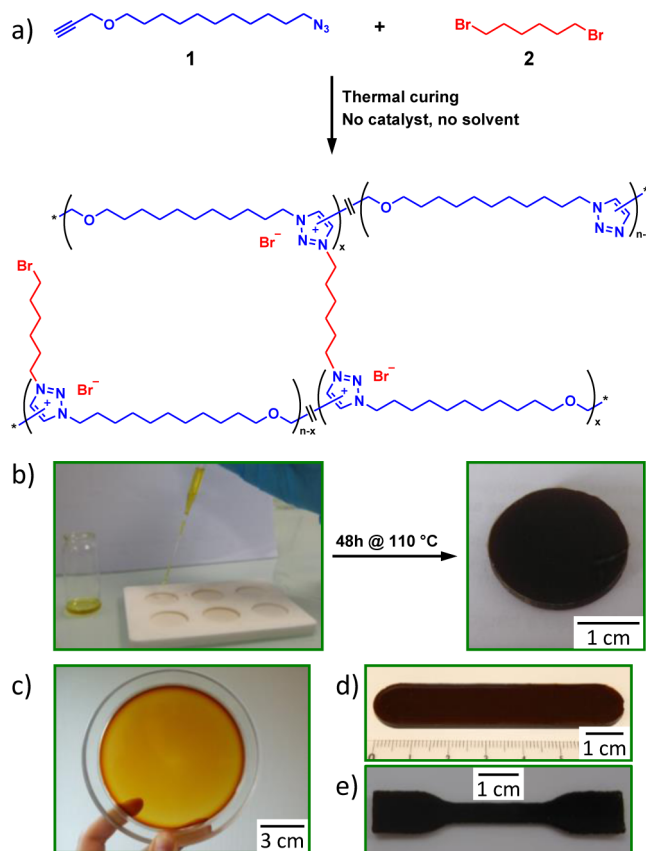


Figure 1. (a) Preparation of ion-conducting networks by simultaneous polyaddition of **1** and cross-linking of the resulting poly(1,2,3-triazole) by difunctional quaternizing agent **2**; (b–e) the low viscosity of the neutral mixture of precursors enables mold-curing samples with a wide range of thicknesses (ranging here from (c) 100 μm for the transparent supported membrane to 2 mm for the samples for (b) rheology or (d,e) mechanical analysis).

triazolium segments containing bromide-functionalized dangling chains, and 63 wt % of segments bridging two 1,2,3-triazolium groups. The remaining 4.0 wt % is the soluble fraction consisting of unreacted cross-linker **2**.

The ionic network obtained from **1** and **2** exhibits a glass transition temperature (T_g) of -11 °C and a storage modulus at the rubbery plateau (E'_g) of approximately 10 MPa (Figures S6 and S7 and Table S1, Supporting Information). The versatility of this cross-linking approach is illustrated by its ability to provide PTIL networks using other monomers and cross-linking agents such as 1,8-diiodooctane (**3**) and triethylene glycol bismesylate (**4**) (Scheme S1, Supporting Information). Notably, the T_g can be increased by changing the counteranion from bromide to iodide or decreased by using a more flexible triethylene glycol cross-linker in conjunction with a mesylate counteranion. The thermal stability of the PTIL networks is comparably high ($T_{\text{d}10}$ ranges from 235 to 247 °C) for all cross-linkers and counteranions investigated (Figure S8, Supporting Information). All cured networks are insoluble in water and common organic solvents. Extended immersions at temperatures ranging from 20 to 110 °C induce moderate swelling ($1/q_2$ ranges from 1.2 to 2.7), and the soluble fraction remains low (w_s ranges from 2.3% to 5.1%) in close agreement to the amount of non-cross-linked reagents determined by XPS (Table S2, Supporting Information). In contrast, the networks behave entirely different when exposed to an excess of

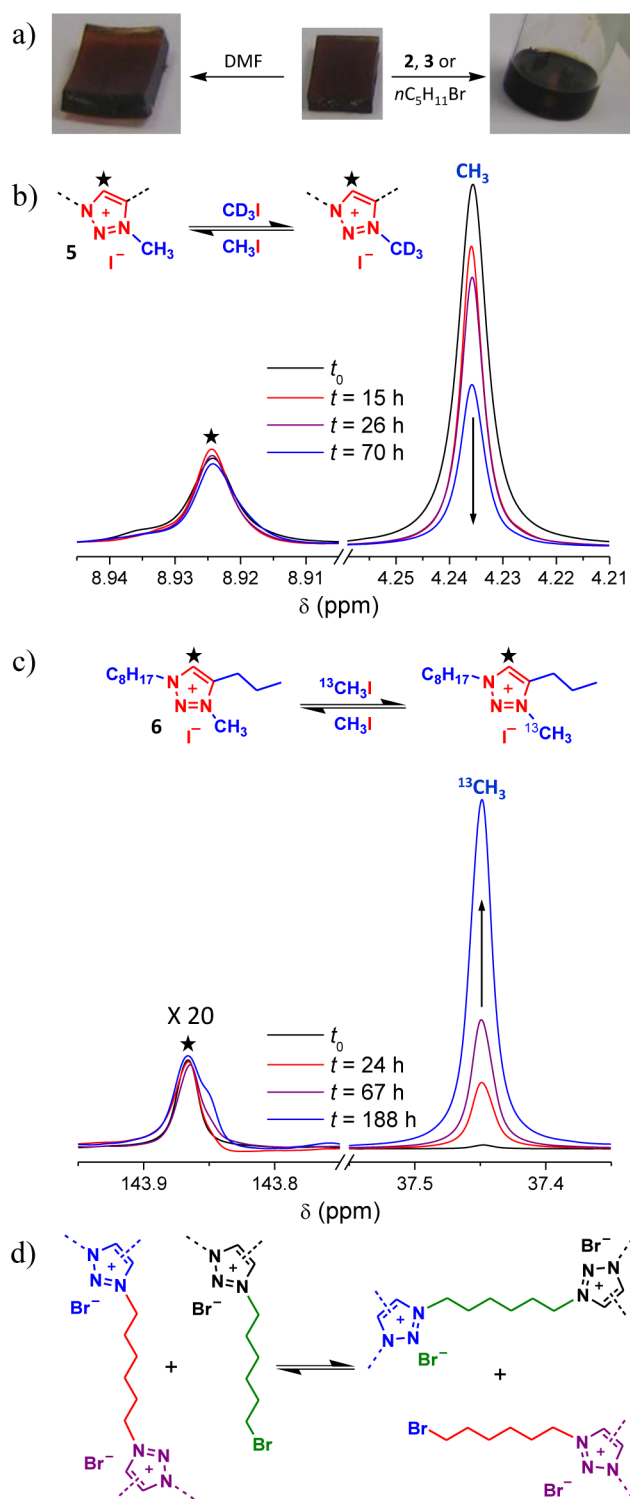


Figure 2. (a) Optical images of the swelling in DMF (left) and the dissolution in **2** (right) of an equilibrated network (middle); (b) ^1H NMR (DMSO- d_6) monitoring of the transalkylation in DMF between CD_3I and linear poly(3-methyl-1,2,3-triazolium) **5**; (c) ^{13}C NMR (DMSO- d_6) monitoring of the transalkylation in bulk between $^{13}\text{CH}_3\text{I}$ and 1,2,3-triazolium ionic liquid **6**; (d) proposed mechanism for the transalkylation reaction.

halogenated hydrocarbons such as 1-bromopentane or dihalogenated monomers **2** and **3**. Complete dissolution is attained within 24–96 h at 110 °C (Figure 2a).

Given the stability of 1,2,3-triazolium cross-links in other solvents, this intriguing behavior points out a possible transalkylation reaction between 1,2,3-triazoliums and alkyl halides, where the elastically active substituent at the *N*-3 position of 1,2,3-triazolium cross-links could be exchanged for an elastically inactive alkyl group until only 1,2,3-triazolium-based ionic liquids remain. Transalkylation reactions of this nature remain vastly unexplored, although compelling evidence has been gathered for imidazolium ionic liquids²⁷ or quaternary ammonium salts.^{28,29} The transalkylation reaction was monitored by ^1H and ^{13}C NMR spectroscopy using as model compounds linear PTIL **5** (obtained by CuAAC polyaddition of **1** and quantitative quaternization with CH_3I)³⁰ and 1,2,3-triazolium ionic liquid **6** (Scheme 1, Supporting Information). PTIL **5** was heated for 70 h at 110 °C in DMF in the presence of a large excess of deuterated iodomethane (CD_3I). ^1H NMR monitoring of the resulting PTIL isolated at different reaction times (Figure 2b) indicates the gradual decrease of the signal at 4.24 ppm associated with the progressive substitution of CH_3 located at the *N*-3 position of the 1,2,3-triazolium groups with CD_3 . In order to rule out a possible lability of the weakly acidic CH_3 protons and to make sure that this substitution is solely due to a C–N bond exchange, we have also monitored by quantitative ^{13}C NMR spectroscopy the transalkylation process by heating for 188 h at 110 °C in the bulk a mixture of 1,2,3-triazolium ionic liquid **6** in the presence of a large excess of ^{13}C -labeled iodomethane ($^{13}\text{CH}_3\text{I}$). The strong increase of the signal at 37.45 ppm (Figure 2c) corroborates the replacement of CH_3 groups at the *N*-3 position by $^{13}\text{CH}_3$ and undoubtedly confirms that transalkylations are effectively taking place by covalent exchanges of C–N bonds. In both experiments, the 1,2,3-triazolium signals remain constant, and there is no evidence of the formation of 1,2,3-triazole groups by dealkylation or elimination reactions at 110 °C.

If transposed to bulk materials, in situ transalkylation reactions should act as exchangeable covalent cross-links (Figure 2d) and provide to ion-conducting PTIL networks the unique viscoelastic properties of vitrimers.¹⁰ The ability to flow and relax stresses by reshuffling the 1,2,3-triazolium cross-links was first investigated by stress relaxation experiments on poly(1,2,3-triazolium bromide) networks (Figure 3a). The networks are effectively able to relax stresses following a single relaxation decay, and the characteristic relaxation time (τ^*) ranges from half an hour at 130 °C to a few seconds at 200 °C. In a similar manner to polyester networks exchanging cross-links by transesterification reactions,^{4,8–13} τ^* of PTIL networks follows Arrhenian variations as the mechanical relaxation is driven by the transalkylation chemical exchange. The viscosity dependence with temperature is plotted in Figure 3b using the Angell fragility plot convention.³¹ Reciprocal temperatures are normalized by a freezing transition temperature ($T_{\text{freeze}} = 98$ °C) extrapolated so that $\eta(T_{\text{freeze}}) = 10^{12}$ Pa·s (Figure S9, Supporting Information). The PTIL networks display a typical behavior of strong glass former with a viscosity activation energy (E_a) of 140 kJ mol^{-1} (Figure S10, Supporting Information), just as in the case of silica glass and other vitrimers but in striking contrast to conventional linear polymers such as polystyrene.^{31,32}

The ability to relax stresses is not limited to small deformations, but can be extensively employed to reprocess the material when the temperature and deformation rates are carefully matched. Similarly to any other highly cross-linked network such as epoxy–amine thermosets, the PTIL networks

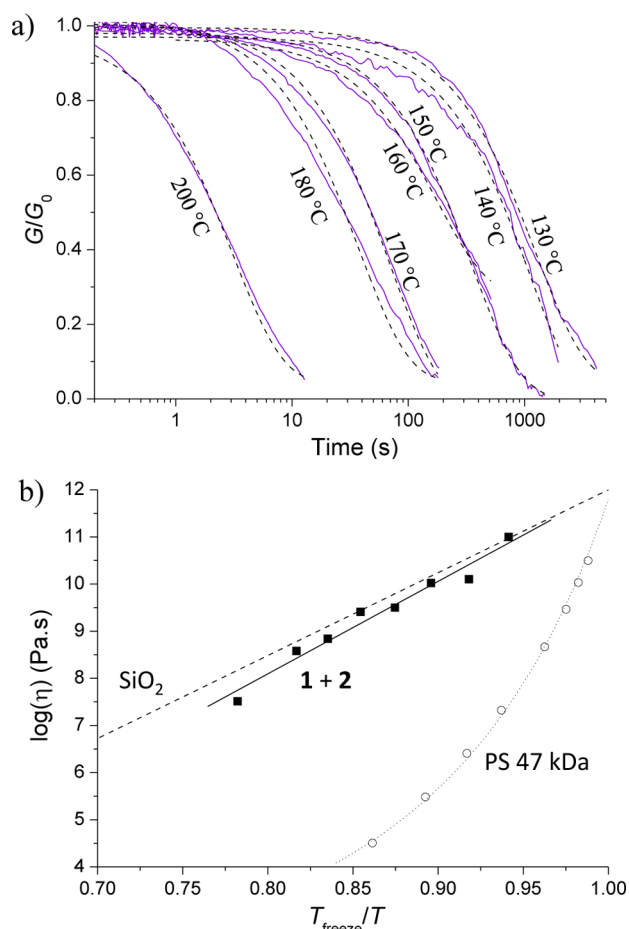


Figure 3. Rheological study of the stress relaxation of ion-conducting poly(1,2,3-triazolium bromide) networks obtained from 1 + 2. (a) Normalized stress relaxation at different temperatures; (b) Angell fragility plot showing viscosity as a function of reciprocal temperature normalized to 1 at the topology freezing transition temperature for ion-conducting PTIL network 1 + 2 ($T_{\text{freeze}} = 98^\circ\text{C}$, solid squares), silica²⁹ (dotted line), and a 47 000 g mol⁻¹ polystyrene³² (open circles).

cannot withstand high deformation (strain at break is $\sim 20\%$, see Figure S14, Supporting Information), and it can be very difficult to bend the material directly in its final shape and then relax the stresses by heat. However, when the deformation rate is slower than the relaxation rate, stresses do not build up, and the material can be deformed plastically to a desirable extent. Creep experiments allowed precise determination of the maximum deformation rate associated with a given stress (Figure S11, Supporting Information). For instance, at 170°C ($\tau^* = 69\text{ s}$), plastic deformation rates up to $1.5\% \text{ min}^{-1}$ can be attained and enable extensive twisting of a planar ribbon into a fusilli-shaped cross-linked PTIL (Figure 4a). It is interesting to note the Newtonian behavior of these PTIL networks as the viscosity determined from creep experiments is independent of the strain rate (Figure S12, Supporting Information). Controlled plastic deformation is in principle applicable to any thermoplastic material. Yet in general, the temperature dependence of viscosity is much stronger for thermoplastics than for vitrimers and strong glass formers (Figure 3b);³² the slightest variation of temperature during deformation dramatically induces inhomogeneous deformation of the material.

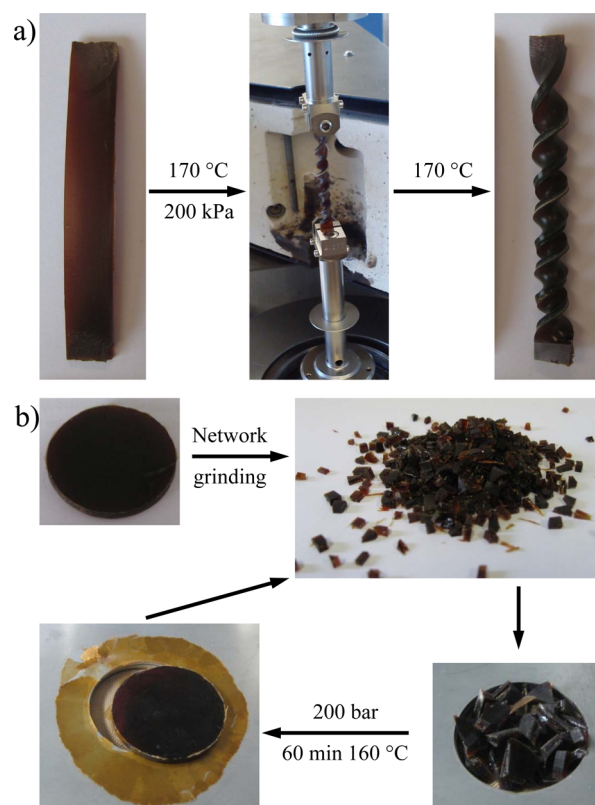


Figure 4. Reshaping and recycling of ion-conducting poly(1,2,3-triazolium bromide) networks obtained from 1 + 2. (a) Demonstration of the vitrimer malleability by reshaping a cross-linked ion-conducting PTIL ribbon into a fusilli-shaped network by applying a constant torque at 170°C . No change in the shape was observed after further heating of the sample at 170°C for 60 min; (b) recycling of an ion-conducting PTIL network by hot pressing.

To demonstrate the tunability of our cross-linking approach, two other series of PTIL networks with different counteranions and chemical structure were prepared using difunctional cross-linkers 3 or 4 in stoichiometric ratios with 1 ($X = 2[3 \text{ or } 4]/[1] = 1.0$). While the curing of 1 + 3 proceeds similarly to 1 + 2 in terms of reaction kinetics at 110°C , the curing of 1 + 4 is significantly slower and has to be performed at 125°C in order to obtain a comparable t_{gel} . The stress relaxation kinetics of PTIL networks are clearly affected by the nature of the counteranions and by the chemical structure of the cross-links as highlighted by stress relaxation experiments performed at 150°C for the three different networks (Figure S13, Supporting Information). While bromide-containing network 1 + 2 and iodide-containing network 1 + 3 have τ^* values of 347 and 1030 s, respectively, the mesylate-containing network 1 + 4 flows extremely slowly ($\tau^* = 180\,000\text{ s}$) and might be difficult to reprocess extensively below 200°C while higher temperatures would most probably damage the network structure and induce undesirable side reactions. These structural effects could also be observed in the network dissolution experiments (Table S2, Supporting Information), that is, dissolution of a bromide-containing network is faster with a brominated alkane than with an iodinated alkane. The respective effects of counteranion and chemical natures of the monomer and cross-linker on the transalkylation reaction is still to be studied in greater detail.

The recyclability of ion-conducting PTIL networks **1 + 2** or **1 + 3** could be considered as a consequence of extensive plastic deformation at high temperature under load. As an example, samples of PTIL networks obtained from **1 + 3** were cut into 2–3 mm pieces and compression molded at 160 °C for 60 min (Figure 4b). Samples obtained after one and two recycling cycles had a defect-free appearance as well as the same extension at break of approximately 20% that denotes an efficient rebonding of the fragments (Figure S14, Supporting Information). However, there was a decrease in Young's modulus (E) from 8 to 4 and 3 MPa after the first and second reprocessing steps. Several hypotheses could explain this undesirable loss of mechanical properties. Occurrence of chain-scission side reactions during prolonged heating at high temperature (at 160 °C, 1 h long recycling steps represent ~14-times the relaxation time) could be one of them. However, these reactions could not be evidenced by thermogravimetric analysis–mass spectrometry (TGA-MS). The most likely explanation comes from the irreversible scission of covalent bonds when the ground samples are reprocessed using high pressure. In-depth studies of composition, macromolecular architecture, and processing conditions will allow decreasing of the degradation of PTIL networks and enhancement of the mechanical properties after recycling, for example, by reducing the recycling times, the applied pressure, or the reprocessing temperatures.

PTIL networks represent the first example of functional vitrimer materials as they display, in addition to good mechanical and reprocessing properties, highly valuable ion-conducting properties. Poly(ionic liquid)s have a bright future as high-strength solid electrolytes able to substitute liquid electrolytes in a broad range of applications. Ion-conducting properties under anhydrous conditions were thus assessed by broadband dielectric spectroscopy (Figure S15, Supporting Information). For each type of network, the ionic conductivity (σ_{DC}) follows a typical Vogel–Fulcher–Tammann dependence due to the correlation between the charge transport of the ionic species and the segmental mobility of the polymer matrix. σ_{DC} is significantly impacted by the chemical nature of the cross-linker and the counteranion since a 3 orders of magnitude decrease in σ_{DC} is observed at room temperature in the following order **1 + 2** > **1 + 4** \gg **1 + 3**. The highest level of anhydrous ionic conductivity ($\sigma_{DC} = 2 \times 10^{-8} \text{ S cm}^{-1}$ at 30 °C) is obtained for the bromide anion. This is typical of nondoped cross-linked ionic networks and is due to the reduced mobility of the ion pairs compared to linear PILs ($\sigma_{DC} < 10^{-5} \text{ S cm}^{-1}$ at 30 °C) or ILs ($\sigma_{DC} < 10^{-2} \text{ S cm}^{-1}$ at 30 °C). Remarkably, the high content of ionic species allows doping readily of the σ_{DC} of the networks using ionic salts or ionic liquids. The impacts of the ratio and structural parameters of the building blocks and the addition of ion-conducting dopants is actually under study and will be reported shortly.

CONCLUSION

Transalkylation covalent exchanges occurring in 1,2,3-triazolium-based cross-linked networks open highly valuable features of malleability, reprocessability, and recycling to ion-conducting solid electrolytes. This may prove particularly interesting in the solvent-free processing of polyelectrolyte membranes and in the development of recyclable or self-healing solid electrolytes with significant opportunities in applications such as batteries, supercapacitors, or membranes for fuel cells and CO₂ recovery. In addition, optical, mechanical, or ion-conducting properties of

the PTIL networks can be readily adjusted by the addition of different organic or inorganic fillers in the initial curable mixture. Alternatively, studying and improving transalkylation exchanges in imidazolium or ammonium-based materials and ionic liquids might prove a formidable tool to synthesize new materials and further develop the field of functional vitrimers.

ASSOCIATED CONTENT

Supporting Information

Further details for all experiments discussed here including synthetic methods and characterizations by differential scanning calorimetry, TGA, dynamic mechanical analysis, XPS, stress relaxation, creep, tensile testing, and ionic conductivity measurements. The Supporting Information is available free of charge on the ACS Publications website at DOI: 10.1021/jacs.5b02653.

AUTHOR INFORMATION

Corresponding Authors

*damien.montarnal@univ-lyon1.fr

*eric.drockenmuller@univ-lyon1.fr

Notes

The authors declare no competing financial interest.

ACKNOWLEDGMENTS

Guilhelm Quintard and Laurence Massin are thanked for their assistance with rheology and XPS measurements, respectively. This research was supported by the Agence Nationale de la Recherche (ANR) (contract ANR-12-JS08-0011 (NAMASTE)). E.D. gratefully acknowledges the financial support from the Institut Universitaire de France (IUF).

REFERENCES

- (1) Wojtecki, R. J.; Meador, M. A.; Rowan, S. J. *Nat. Mater.* **2011**, *10*, 14–27.
- (2) Urban, M. W. *Nat. Chem.* **2012**, *4*, 80–82.
- (3) Scott, T. F.; Schneider, A. D.; Cook, W. D.; Bowman, C. N. *Science* **2005**, *308*, 1615–1617.
- (4) Yoon, J. A.; Kamada, J.; Koynov, K.; Mohin, J.; Nicolay, R.; Zhang, Y.; Balazs, A. C.; Kowalewski, T.; Matyjaszewski, K. *Macromolecules* **2012**, *45*, 142–149.
- (5) Kloxin, C. J.; Scott, T. F.; Park, H. Y.; Bowman, C. N. *Adv. Mater.* **2011**, *23*, 1977–1981.
- (6) Pepels, M.; Pilot, I.; Klumperman, B.; Goossens, H. *RSC Polym. Chem.* **2013**, *4*, 4955–4965.
- (7) Oehlenschlaeger, K. K.; Mueller, J. O.; Brandt, J.; Hilf, S.; Lederer, A.; Wilhelm, M.; Graf, R.; Coote, M. L.; Schmidt, F. G.; Barner-Kowollik, C. *Adv. Mater.* **2014**, *26*, 3561–3566.
- (8) Billiet, S.; De Bruycker, K.; Driessen, F.; Goossens, H.; Van Speybroeck, V.; Winne, J. M.; Du Prez, F. E. *Nat. Chem.* **2014**, *6*, 815–821.
- (9) Kloxin, C. J.; Scott, T. F.; Adzima, B. J.; Bowman, C. N. *Macromolecules* **2010**, *43*, 2643–2653.
- (10) Montarnal, D.; Capelot, M.; Tournilhac, F.; Leibler, L. *Science* **2011**, *334*, 965–968.
- (11) Kloxin, C. J.; Bowman, C. N. *Chem. Soc. Rev.* **2013**, *42*, 7161–7173.
- (12) Engle, L.; Wagener, K. J. *Macromol. Sci., Part C: Polym. Rev.* **1993**, *33*, 239–257.
- (13) Maeda, T.; Otsuka, H.; Takahara, A. *Prog. Polym. Sci.* **2009**, *34*, 581–604.
- (14) Capelot, M.; Montarnal, D.; Tournilhac, F.; Leibler, L. *J. Am. Chem. Soc.* **2012**, *134*, 7664–7667.
- (15) Capelot, M.; Unterlass, M. M.; Tournilhac, F.; Leibler, L. *ACS Macro Lett.* **2012**, *1*, 789–792.

- (16) Altuna, F. I.; Pettarin, V.; Williams, J. J. *Green Chem.* **2013**, *15*, 3360–3366.
- (17) Brutman, J. P.; Delgado, P. A.; Hillmyer, M. A. *ACS Macro Lett.* **2014**, *3*, 607–610.
- (18) Pei, Z.; Yang, Y.; Chen, Q.; Terentjev, E. M.; Wei, Y.; Ji, Y. *Nat. Mater.* **2014**, *13*, 36–41.
- (19) Yu, K.; Taynton, P.; Zhang, W.; Dunn, M. L.; Qi, J. *RSC Adv.* **2014**, *4*, 10108–10117.
- (20) Denissen, W.; Rivero, G.; Nicolay, R.; Leibler, L.; Winne, J. M.; Du Prez, F. E. *Adv. Funct. Mater.* **2015**, *25*, 2451–2457.
- (21) Lu, Y.-X.; Guan, Z. *J. Am. Chem. Soc.* **2012**, *134*, 8424–8427.
- (22) Lu, Y.-X.; Tournilhac, F.; Leibler, L.; Guan, Z. *J. Am. Chem. Soc.* **2012**, *134*, 14226–14231.
- (23) Zheng, P.; McCarthy, T. J. *J. Am. Chem. Soc.* **2012**, *134*, 2024–2027.
- (24) Mudraboyina, B. P.; Obadia, M. M.; Allaoua, I.; Sood, R.; Serghei, A.; Drockenmuller, E. *Chem. Mater.* **2014**, *26*, 1720–1726.
- (25) Obadia, M. M.; Mudraboyina, B. P.; Allaoua, I.; Haddane, A.; Montarnal, D.; Serghei, A.; Drockenmuller, E. *Macromol. Rapid Commun.* **2014**, *35*, 794–800.
- (26) Yuan, J.; Mecerreyes, D.; Antonietti, M. *Prog. Polym. Sci.* **2013**, *38*, 1009–1036.
- (27) Meine, N.; Benedito, F.; Rinaldi, R. *Green Chem.* **2010**, *12*, 1711–1714.
- (28) Wilson, R. B.; Laine, R. M. *J. Am. Chem. Soc.* **1985**, *107*, 361–369.
- (29) Leir, C. M.; Stark, J. E. *J. Appl. Polym. Sci.* **1989**, *38*, 1535–1547.
- (30) Dimitrov-Raytchev, P.; Beghdadi, S.; Serghei, A.; Drockenmuller, E. *J. Polym. Sci., Part A: Polym. Chem.* **2013**, *51*, 34–38.
- (31) Angell, C. A. *Science* **1995**, *267*, 1924–1933.
- (32) Plazek, D. J.; O'Rourke, V. M. *J. Polym. Sci., Part A-2* **1971**, *9*, 209–243.